京都大学防災研究所年報　第 47 号 C　平成 16 年
Annuals of Disa. Prev. Res. Inst., Kyoto Univ., No. 47, 2004

Modulation of the stratosphere-troposphere coupling process of the Northern Hemisphere annular mode associated with the ENSO cycle

Hideo SHIOGAMA * and Hitoshi MUKOUGAWA

*COE Researcher, DPRI, Kyoto University

Synopsis

Recent observational studies reveal some evidence that, in intraseasonal time scales, the downward propagation of zonal mean zonal wind anomalies in the stratosphere precedes the Northern Hemisphere annular mode (NAM) signal in the troposphere. In this study, interannual variability of this type of stratosphere-troposphere dynamical coupling in winter was examined by using NCEP/NCAR reanalysis and Met Office HadISST datasets. In particular, we focused upon the dependence of the coupling on the ENSO phase (warm/cold phase).

The downward propagation of zonal wind anomalies in the stratosphere is evident irrespective of the ENSO phase, while the zonal wavenumber (WN) of planetary waves responsible for the zonal wind anomalies is different: WN 2 (WN 1) component plays a primary role in the cold (warm) phase. The region where anomalous upward propagation of wave activity is observed also depends on the ENSO phase: the Eurasian (Pacific-North Atlantic) sector for cold (warm) phase. On the other hand, large tropospheric zonal wind anomalies followed by the stratospheric zonal wind anomalies appear only for the cold phase. Anomalous poleward propagation of wave activity of planetary waves with WN 2 as well as synoptic waves acts to reinforce the tropospheric zonal wind anomalies.

Keywords: annular mode, stratosphere-troposphere coupling, ENSO, sudden warming

1. Introduction

The dominant mode of surface pressure variability between Arctic and mid-latitudes in the boreal cold season has attracted more attention in recent years. The spatial pattern of the dominant mode is characterized by its zonal symmetry, and the mode was named as Northern Hemisphere annular mode (NAM) by Thompson and Wallace (1998, 2000). Such annular structure is observed in the lower stratosphere as well as the troposphere, suggesting dynamical coupling between circulations in the stratosphere and troposphere.

A few studies stressed the non-linear aspects of the NAM, although most studies of the NAM treated its temporal index based on linear paradigm. Quadrelli and Wallace (2002) suggested that year-to-year variability of the NAM is significantly different during warm and cold winters of the El Nino / Southern Oscillation (ENSO) cycle. They showed that the dominant modes of surface pressure variability observed in the warm and cold winters of the ENSO cycle are similar with the North Atlantic Oscillation and the NAM, respectively.

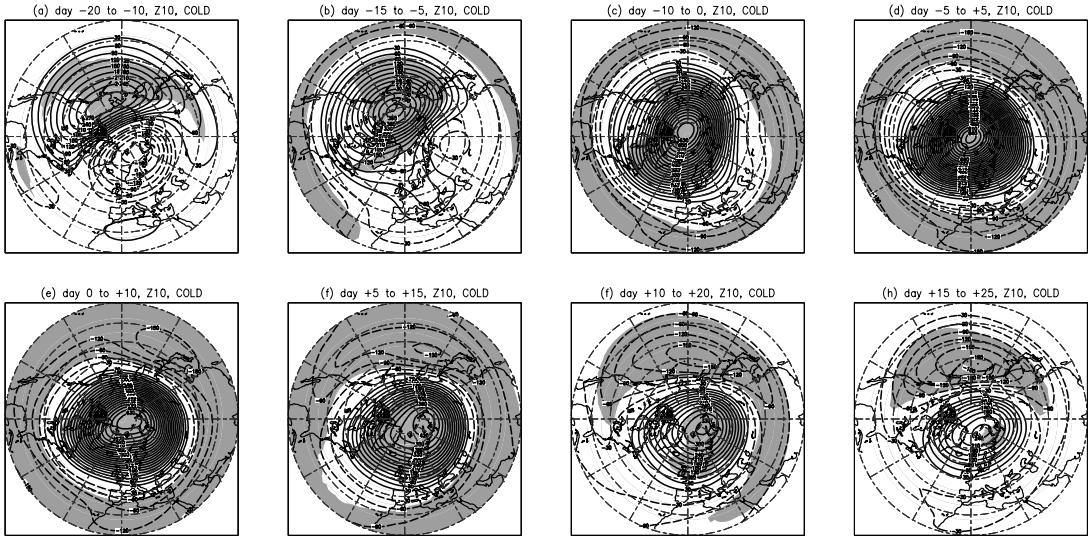

Fig. 1: Height anomalies (contours; m) at 10-hPa temporarily averaged over the periods between (a) day –20 and day –10, (b) day –15 and day –5, (c) day –10 and day 0, (d) day –5 and day +5, (e) day 0 and day +10, (f) day +5 and day +15, (g) day +10 and day +20, (h) day +15 and day +25 of the COLD years. Height anomaly averages are weighted by (sine of 45N / sine of latitude), and are computed after truncation of height anomalies at zonal wavenumber 4. Shading indicates statistically significant anomalies at 95% level, as based on bootstrap test with 1000 times resampling.

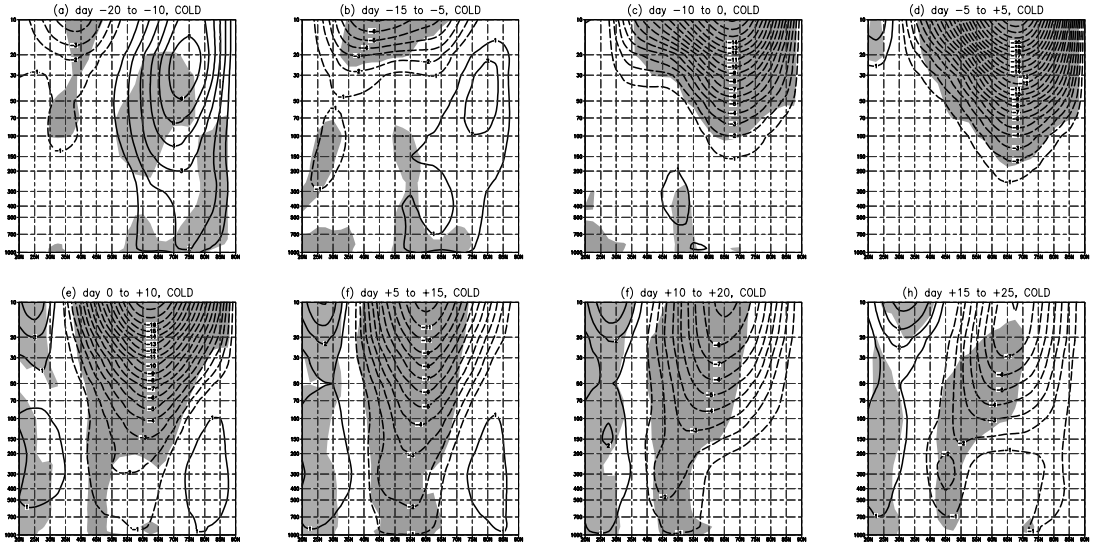

Fig. 2: Same as Fig. 1 except for zonal mean zonal wind anomalies (ms^{-1}) for the COLD years.

On intraseasonal time scales, the NAM signal in the stratosphere or the downward propagation of the zonal mean zonal wind anomalies from the stratosphere precede the NAM signal seen in the troposphere (Kodera et al., 1999; Baldwin and Dunkerton, 1999, 2001). Some observational studies (e.g. Kuroda and Kodera, 1997; Kodera et al., 2000) have shown that enhanced vertical propagation of planetary wave is responsible for the zonal wind anomalies in the stratosphere. It is, however, not clear what mechanism account for the occurrence of the zonal wind anomalies in the troposphere.

The aim of the present study is to examine interannual variability of this type of

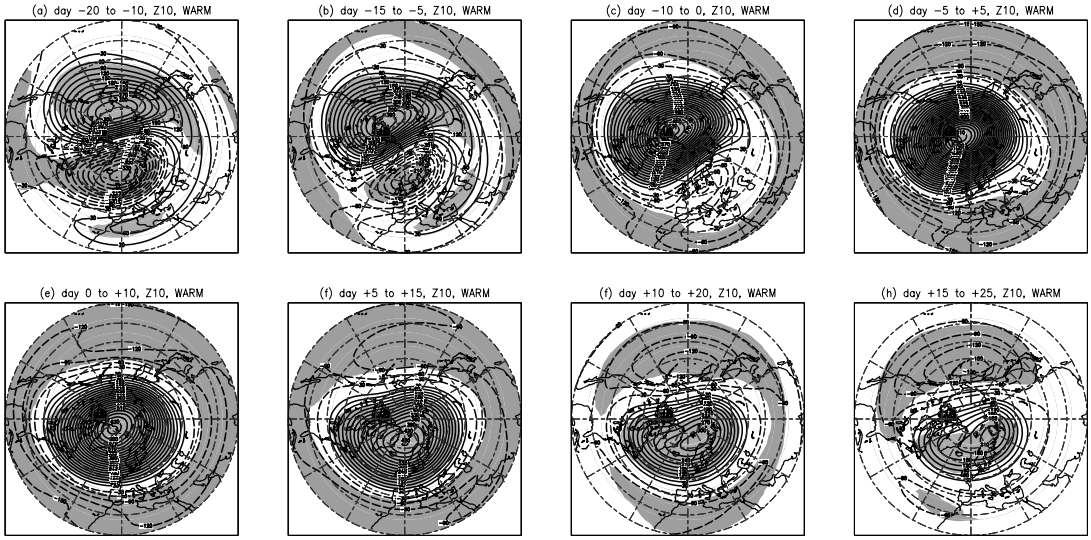

Fig. 3: Same as Fig. 1 except for the WARM years.

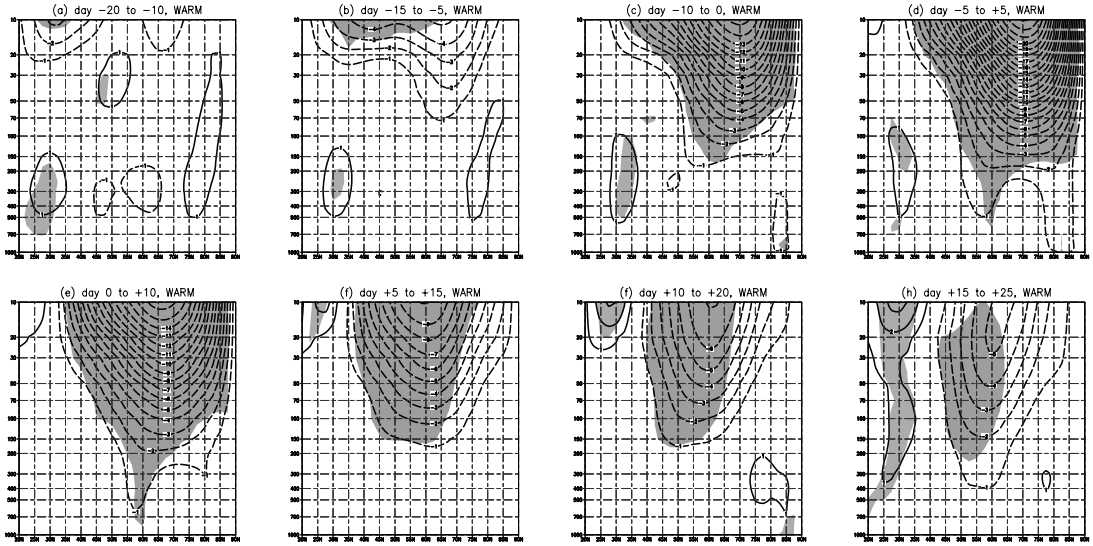

Fig. 4: Same as Fig. 2 except for the WARM years.

stratosphere-troposphere dynamical coupling. In particular, we will show the dependence of the downward propagation process of the NAM signal on the ENSO phase (warm/cold phase). A possible mechanism for the ENSO influence on the stratosphere-troposphere coupling will be discussed.

2. Data and Methods

The present analyses are based on the National Centers for Environmental Prediction / National Center for Atmospheric Research (NCEP-NCAR) daily reanalysis data (Kalnay et al. 1996) and sea surface temperature data of U.K. Met Office monthly HadISST (Rayner et al. 2003) for the 45-year period 1957-2001.

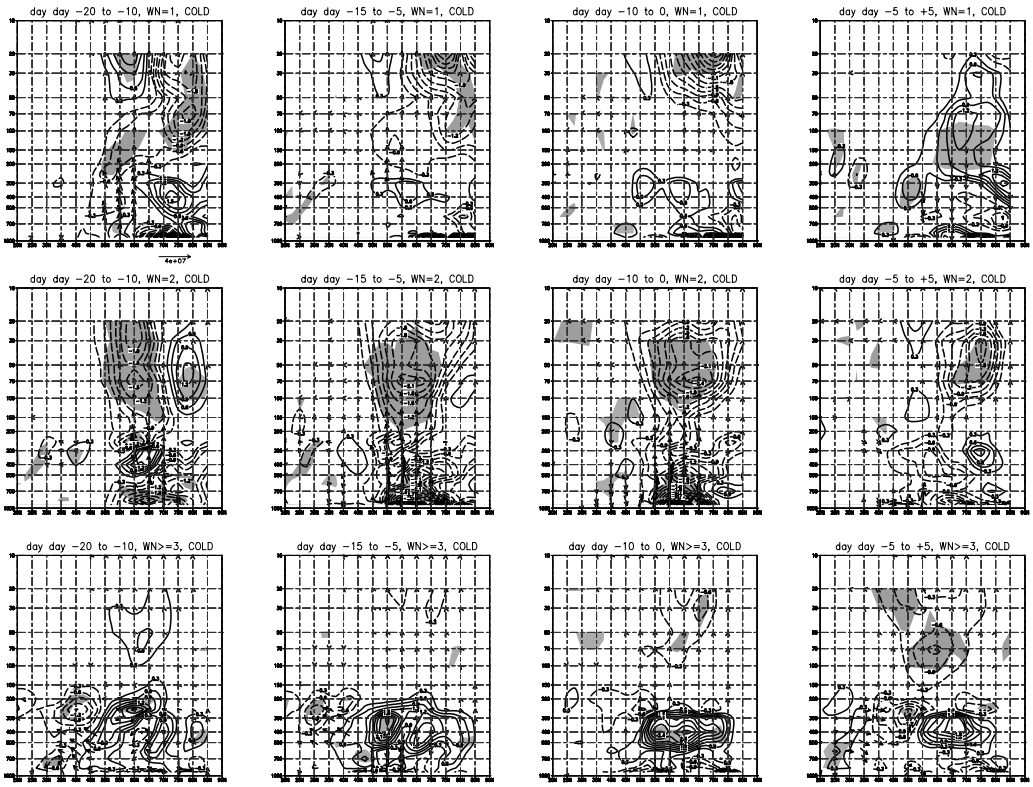

Fig. 5: E-P flux anomalies (vectors; m^2s^{-2}) and divergence anomalies of E-P flux ($ms^{-1}day^{-1}$) of (top panels) WN1, (middle panels) WN2, and (bottom panels) WN≧3 for the COLD years. The divergence anomalies are weighted by 1000-hPa/(pressure × radius of earth × cosine of latitude). Only E-P flux anomalies are drawn when their meridional or vertical components are statistically significant at 95%. Shading indicates statistically significant divergence anomalies at 95% level.

The NCEP-NCAR reanalysis include 17 vertical level data from 1000-hPa to 10-hPa. Monthly mean NCEP-NCAR reanalysis data are computed from daily data. Only the boreal cold season (November to April) data are used.

For defining the state of the ENSO cycle we used the cold season mean SST averaged over the area 5.5N-5.5S, 179.5W-90.5W. The NCEP-NCAR reanalysis data of 44 boreal cold seasons were partitioned into 15 warmest (1958, 1966, 1969, 1970, 1973, 1977, 1978, 1980, 1983, 1987, 1988, 1992, 1993, 1995, and 1998) and coldest (1965, 1967, 1968, 1971, 1974, 1975, 1976, 1984, 1985, 1986, 1989, 1996, 1999, 2000, and 2001) years of the ENSO cycle like as Quadrelli and Wallace (2002).

To construct anomalies, at first, the long-term mean daily climatology is calculated in each warm or cold composite. The long-term mean climatology time series, which are additionally 10-day low-pass filtered, are removed. The Lonczos temporal filter (Duchon, 1979) is used in the present study. Next, year-to-year fluctuations of the anomalies, which are each cold season mean, are subtracted to make intraseasonal anomalies. The monthly mean intraseasonal anomalies are formed by similar procedure from the monthly mean data. In the present study, 10-day low-passed and 10-day high-passed anomalies are referred to as low-frequency and high-frequency anomalies, respectively.

To study variations of the polar vortex, the present study uses the index of NAM at 10-hPa. The principal mode of empirical orthogonal function analysis of the monthly Z10 anomalies is computed.

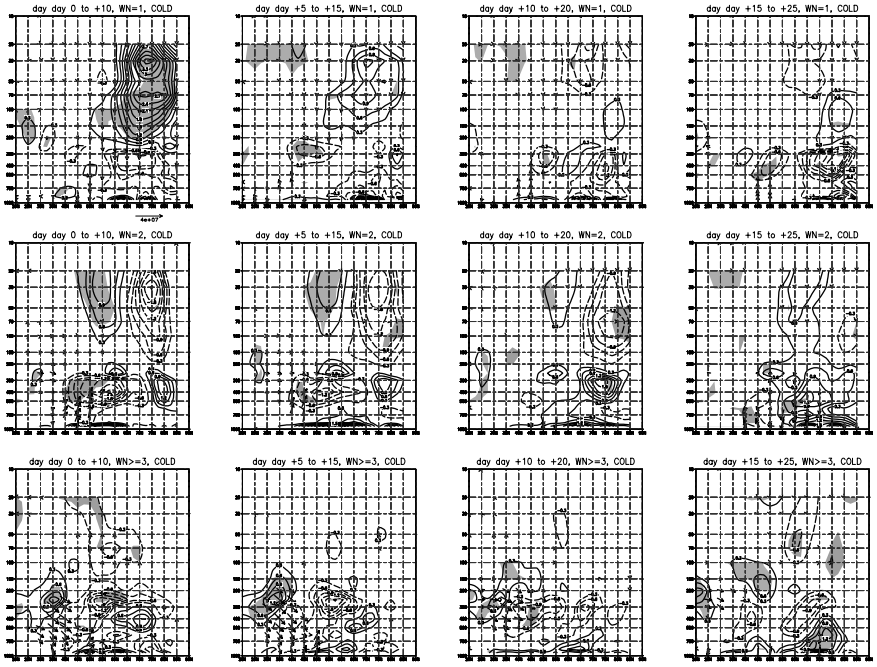

Fig. 5: (Continued)

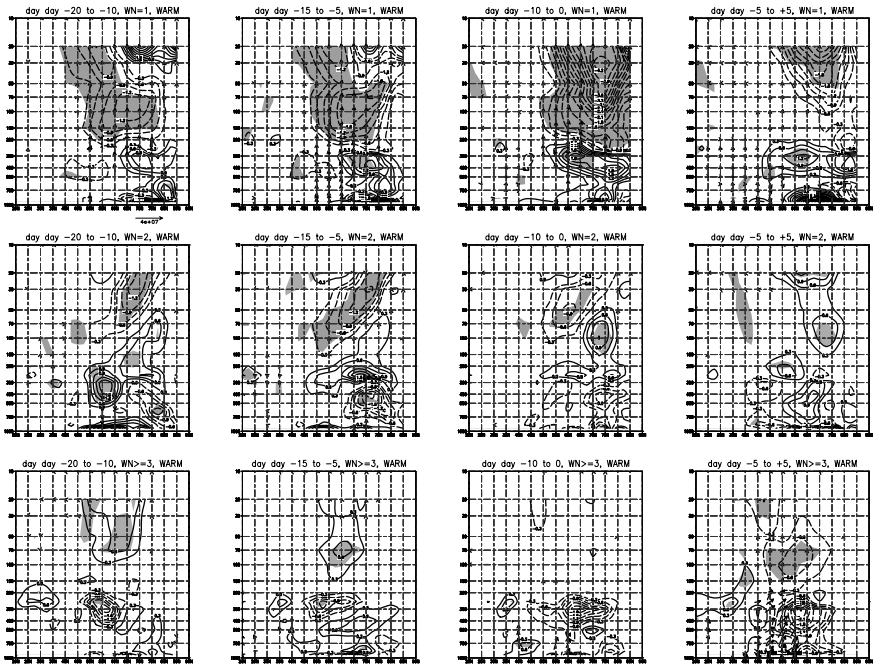

Fig. 6: Same as Fig.5 except for the WARM years.

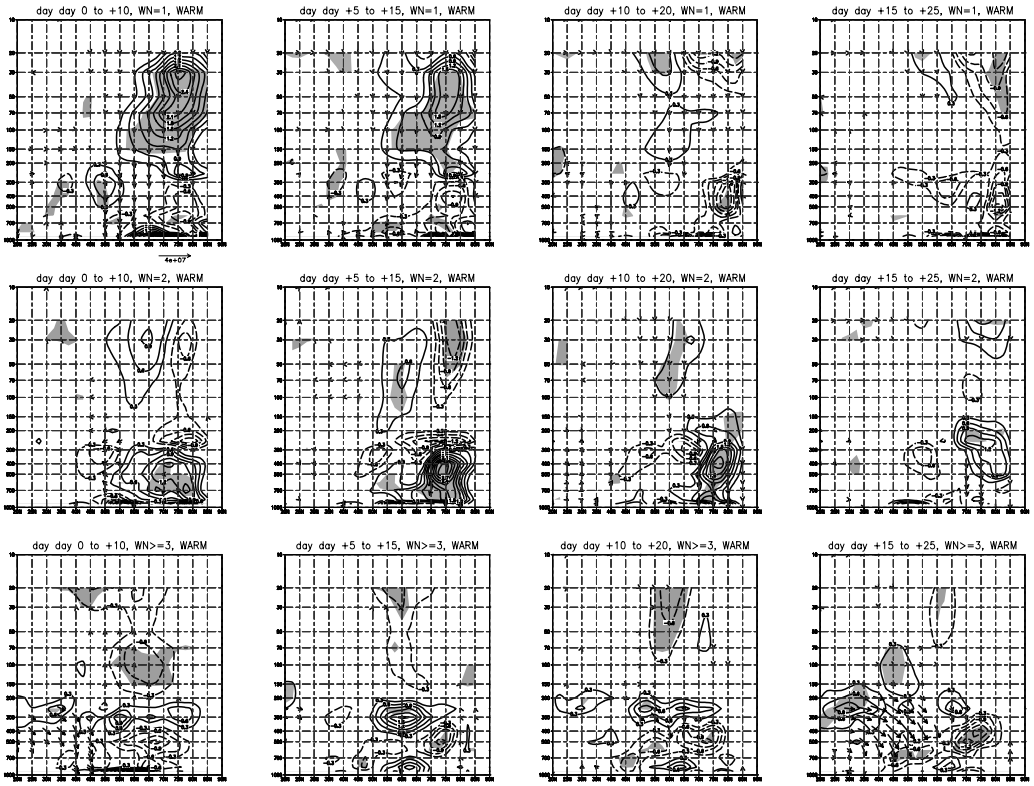

Fig. 6: (continued)

Daily values of NAM index at 10-hPa are calculated by projecting the daily low-frequency Z10 anomalies onto the principal mode. To find events of the weakened polar vortex, we search the durations between the day that the NAM index drops below –1.0 standard deviations and when it rises again above –1.0 standard deviations. The first days when the NAM index reaches minimum values are defined as key-days. If the key-days are found in November or April, they are removed. When some key-days are observed within 60 day duration, only the first day is considered as key-day. There are 18 and 14 key-days in the warm and cold years, respectively. Hereafter all composites are centered about the key-days (referred to as day 0).

When the height anomaly composite maps are constructed, they are computed after truncated at zonal wavenumber 4.

Wave propagation in the zonal mean field and their feedback onto the zonal mean zonal flow are examined with E-P flux (e.g., Andrews et al., 1987). To investigate wave propagation of low-frequency eddies on the zonally varying field, wave activity flux formulated by Takaya and Nakamura (1997, 2001) is calculated.

The geopotential height tendency induced by the high-frequency eddy forcing is diagnosed by computing the convergence of the relative vorticity due to high-frequency eddies (Holopainen et al., 1982). This method has the advantage of filtering small-scale noise that pollutes the estimate of zonal flow tendency. The height tendency anomalies are vertically averaged from 850-hPa to 250-hPa.

Robustness of our findings is statistically tested by bootstrap test (Efron, 1979) with 1000 times resampling of 18 and 14 events for the warm and cold years, respectively.

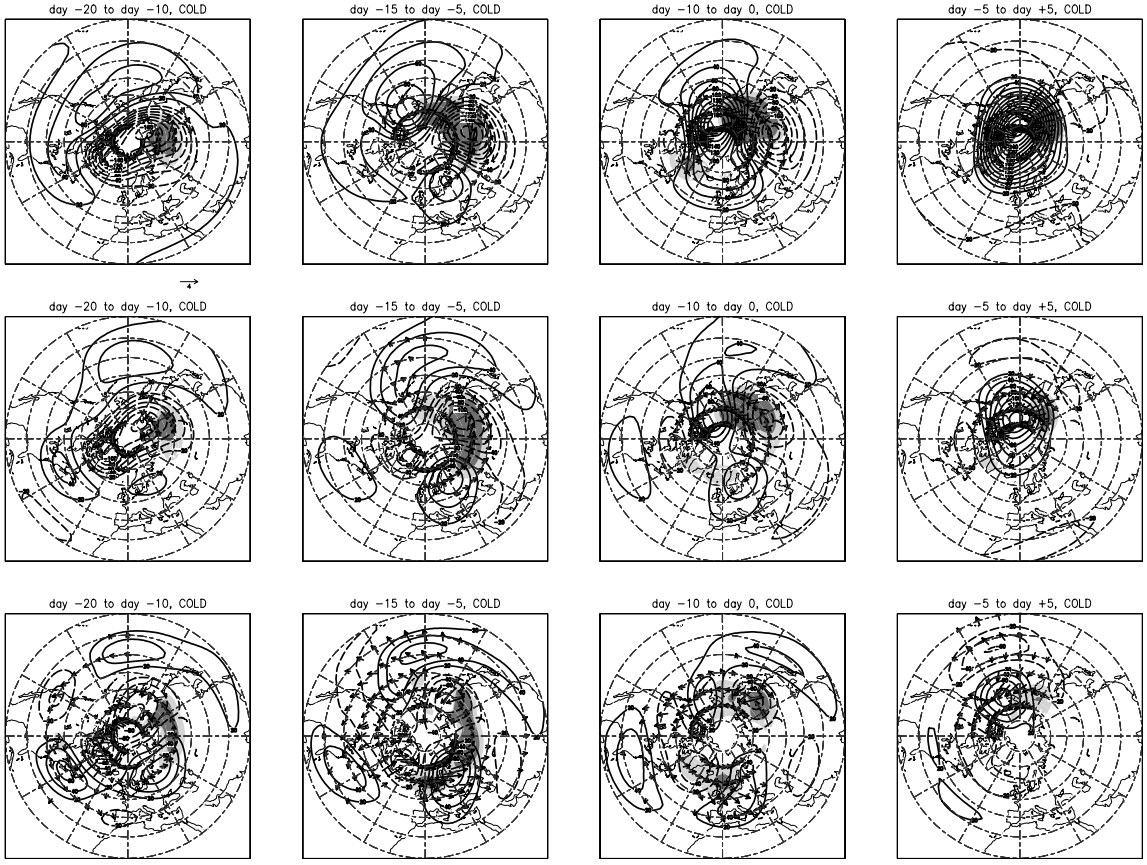

Fig. 7: Height anomalies (contours; m) and horizontal components of wave-activity flux anomaly (vectors) at (top panels) 50-hPa, (middle panels) 100-hPa, and (bottom panels) 250-hPa for the COLD years. Small flux anomalies are not drawn. Shading indicates upwelling components of wave-activity flux anomaly at (top panels) 30-hPa, (middle panels) 70-hPa, and (bottom panels) 200-hPa.

3. Results

Figure 1 shows Z10 anomalies for the cold years. Before the key-days, positive height anomalies are amplified and become to cover the pole. From day –15 to day –5, the planetary wave seems to have zonal wavenumber 1 and 2 components. After the key-day, the positive anomalies gradually decay. Progress of zonal mean zonal wind anomalies for the cold years is indicated by Fig. 2. Large negative zonal wind anomalies first appear in the subtropics. Their information slowly propagate poleward and downward into the troposphere by day +10. In the troposphere, the negative zonal wind anomalies persist until day +20.

In the warm years, positive height anomalies, which seem to be a planetary wave of zonal wavenumber 1, amplify and weaken the polar vortex (Fig. 3). After the key-day, the positive anomalies decay. These results are generally in agreement with that of earlier studies (e.g., Kodera et al., 2000).

Figure 4 shows zonal mean zonal wind anomalies. Negative zonal wind anomalies propagate poleward and downward. However, little negative zonal wind anomalies are observed in the troposphere. It is interest finding that troposheric aspect of the stratosphere-troposphere coupling process of the NAM is different between the cold and warm years of the ENSO cycle.

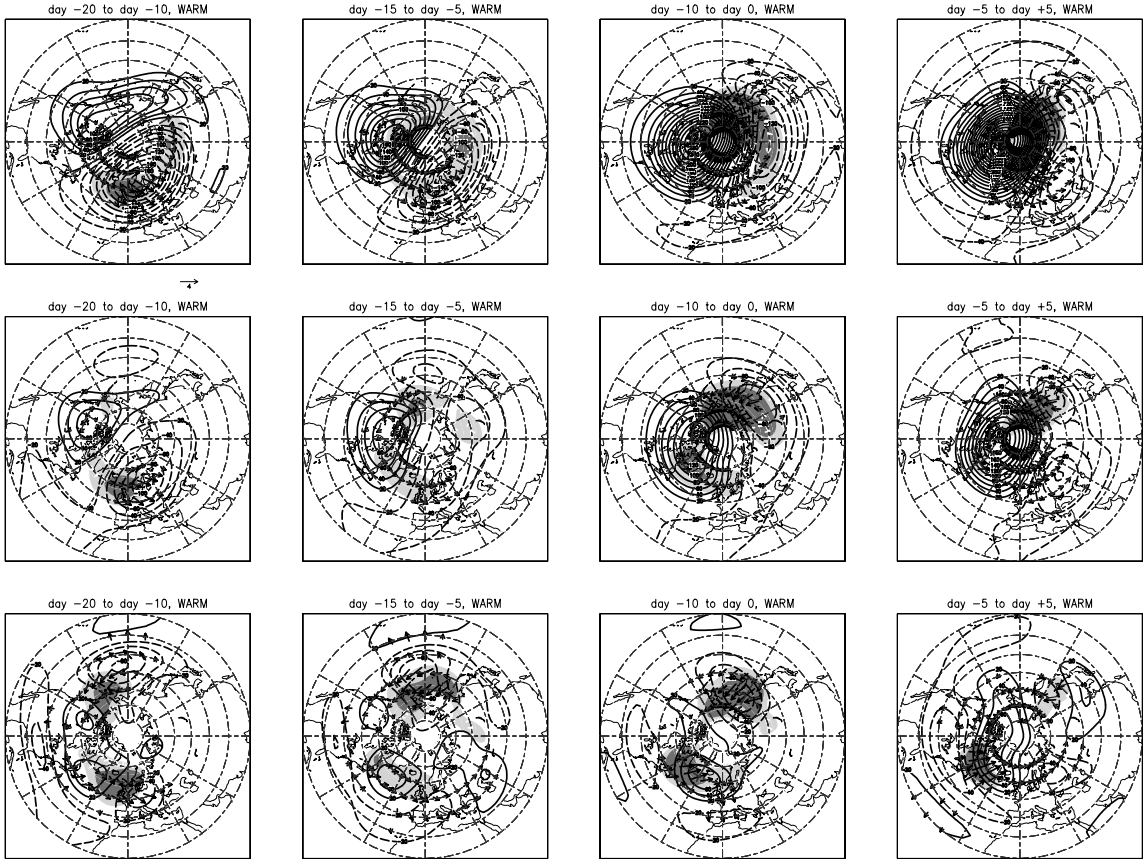

Fig. 8: Same as Fig. 7 except for the WARM years.

In the earlier stage of the events, anomalous upward propagation of planetary waves should contribute to the downward extension of the negative zonal wind anomalies in the stratosphere (e.g., Kuroda and Kodera, 1999).

Propagation of wave and its action onto the zonal mean zonal wind on the zonal mean field is diagnosed by E-P flux anomalies and its divergence anomalies (Figs. 5 and 6).

In the earlier stage of the cold year events, planetary waves of zonal wavenumber 2 are more important than ones of wavenumber 1 in the contribution to the decelerations of zonal mean westerly in the stratosphere. After the key-day of the cold year events, poleward propagation anomalies of WN2 and higher wavenumber eddies are responsible to deceleration of westerly in the mid-latitude of troposphere. On the other hand, in the earlier stage of warm year events, upward propagation of planetary waves of zonal wavenumber 1 dominates. In the later stage, little significant westerly tendency anomalies are observed. These differences of wave action in the troposphere between the cold and warm years account for the different progress of zonal wind anomalies observed in the troposphere.

Comparisons between structure of wave and wave propagation are made in Figs. 7 and 8. Vectors are wave flux anomalies formulated by Takaya and Nakamura (1997, 2001). Shading indicates upward flux anomalies. In the earlier stage, there is a difference between the sectors of longitude where upward wave activity flux anomalies are observed.

In the cold years, the enhanced vertical propagation of wave packets occurs over the Eurasian sector. This result resembles that of Kuroda and Kodera (1999). At the upper troposphere, these upward wave activity flux anomalies are emitted from the Rossby wave train with horizontal wavelength of 2 over the Eurasian sector. The positive height anomalies at 30E may be blocking anticyclones. On the other hand, in the warm years, upward wave activity flux anomalies are found over

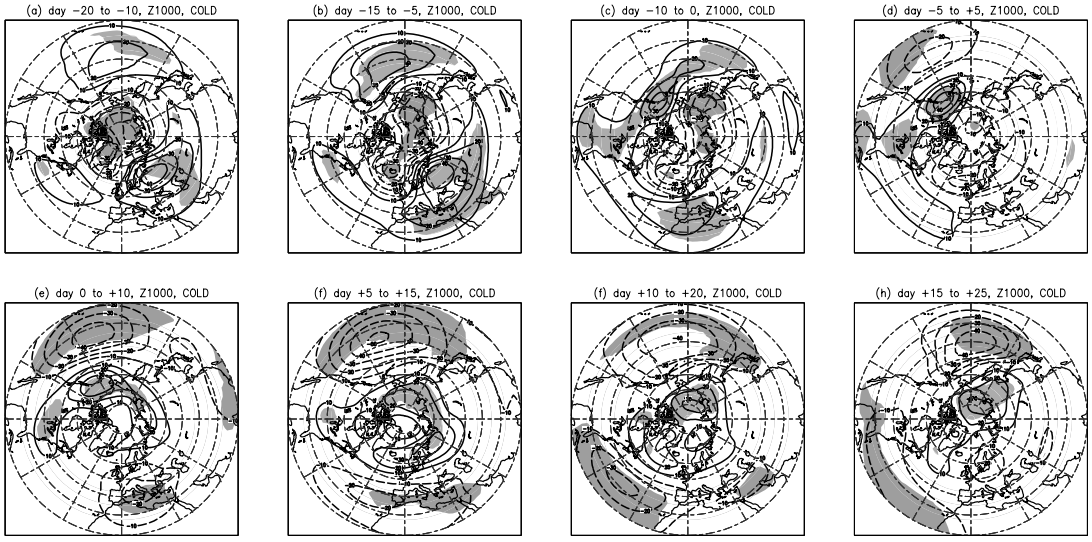

Fig. 9: Same as Fig. 1 except for height anomalies (m) at 1000-hPa for the COLD years.

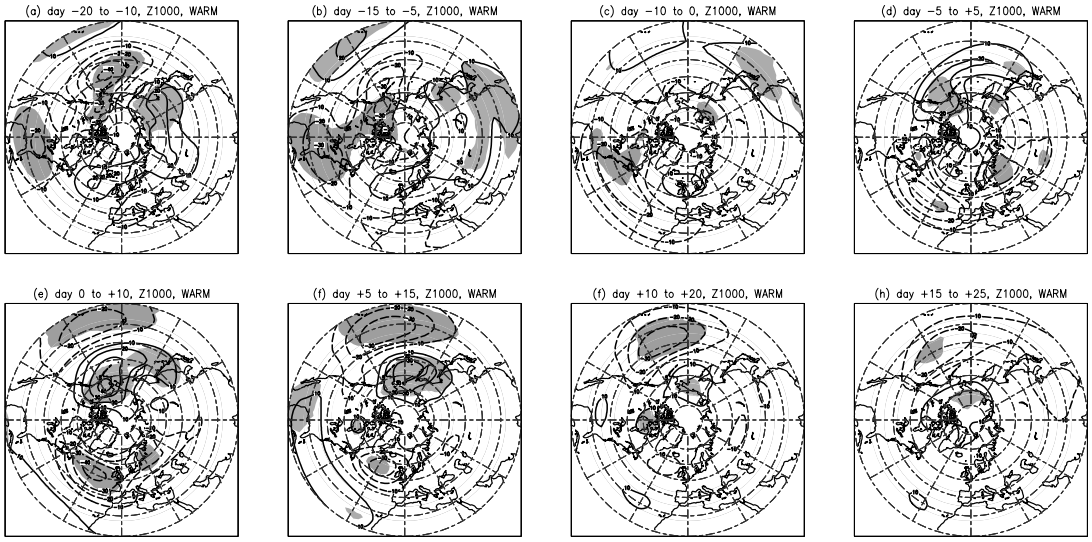

Fig. 10: Same as Fig. 9 except for the WARM years.

the Pacific-North Atlantic sector. This enhanced vertical flux anomalies are accompanied by the Pacific North Atlantic teleconnection patterns. This upward wave packet propagation is responsible for that planetary waves of zonal wavenumber 1 occur in the stratosphere.

Near the surface, in the later stage of the cold year events, the NAM like height anomaly patterns appear (Fig. 9). In the later stage of the warm year events, there is no NAM like anomaly pattern. Dipole anomaly pattern is found in the Pacific Ocean, indicating decelerations of the Pacific jet stream (Fig. 10). On the other hand, negative height anomalies over the higher latitudes of the Atlantic Ocean accompany the accelerations of the Atlantic jet stream.

These differences of height anomalies near the surface in the later stage are associated with height tendency anomalies due to high-frequency eddy. In the cold year events, high-frequency eddy forcing anomalies force the negative height anomalies over the mid-latitudes sectors of the Pacific Ocean and

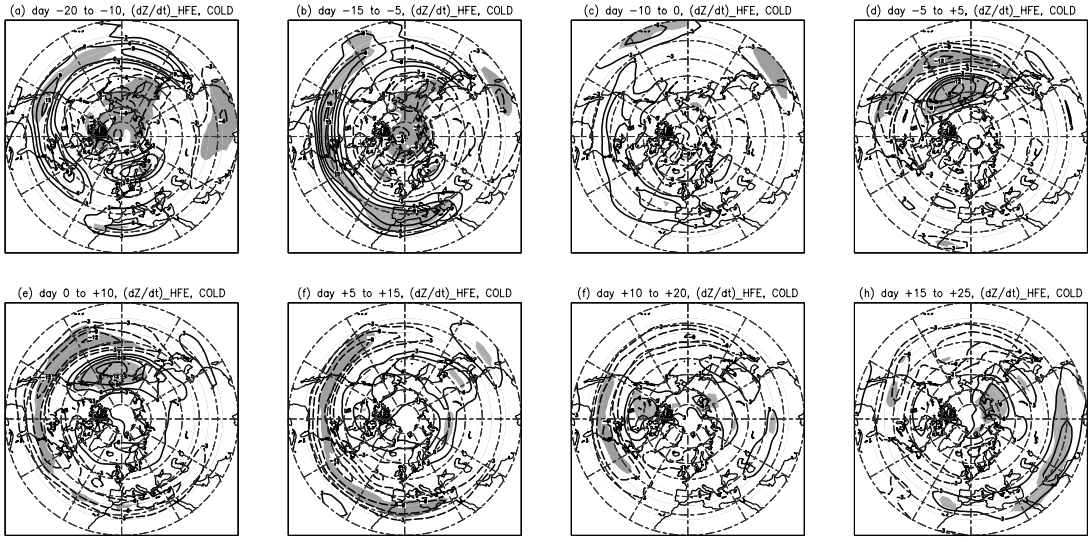

Fig. 11: Same as Fig. 1 except for height tendency anomalies ($mday^{-1}$) due to high-frequency eddies for the COLD years. They are which are vertically averaged from 850-hPa to 250-hPa, and are weighted by (sine of 45N / sine of latitude). Shading indicates statistically significant anomalies at 95% level.

Atlantic Ocean, and positive tendency anomalies over the higher latitudes of the Pacific Ocean, decelerating ambient westerlies from the Pacific Ocean to the Atlantic Ocean. In the warm year events, little high-frequency eddy forcing anomalies is found over the Atlantic Ocean, although dipole pattern of height tendency anomaly is observed in the Pacific Ocean, inducing easterly wind anomalies.

4. Summary

Some studies recently suggest that, in intraseasonal time scales, the downward propagation of zonal mean zonal wind anomalies from the stratosphere appears to precede the Northern Hemisphere annular mode (NAM) signal in the troposphere. The purpose of the present study is to investigate whether the stratosphere-troposphere coupling process of the NAM is different between warm and cold winters of the El Nino and Southern Oscillation by analyzing 44 cold season's datasets of NCEP-NCAR reanalysis and Met Office HadISST.

In the stratosphere downward propagation of zonal wind anomalies is observed during both the warm and cold winters. Upward E-P flux anomalies due to planetary waves of zonal wavenumber 2 and 1 are responsible for the weakening of the polar vortex during the cold and warm winters, respectively. Upward wave activity flux anomalies occur over the Eurasian sector in the cold winters. On the other hand, in the warm winters, anomalous wave activity fluxes are observed over the Pacific-North Atlantic sector.

When the zonal wind anomalies descend to near the tropopause, large zonal wind anomalies appear in the troposphere only during the cold winters. Anomalous poleward E-P fluxes of zonal wavenumber 2 and higher wavenumber seem to decelerate westerlies in the mid-latitudes of the troposphere.

These differences of zonal wind anomalies near the surface in the later stage are associated with high-frequency eddy forcing anomalies. In the cold year events, high-frequency eddy forcing anomalies decelerate the ambient westerlies from the Pacific Ocean to the Atlantic Ocean. In the warm year events, little high-frequency eddy forcing anomalies is found over the Atlantic Ocean, while easterly wind tendency anomalies are observed in the Pacific Ocean.

References

Andrews, D. G., J. R. Holton, and C. B. Leovy 1987: Middle atmosphere dynamics. Academic Press, New

York. 489 pp

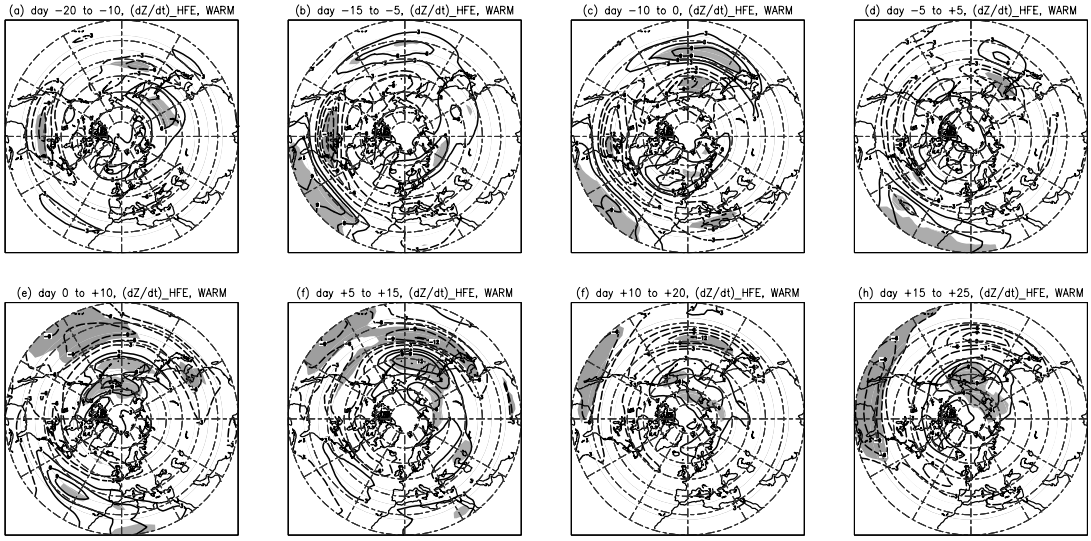

Fig. 12: Same as Fig. 11 except for the WARM years.

Baldwin, M. P., and T. J. Dunkerton, 1999: Propagation of the Arctic Oscillation from the stratosphere to the troposphere. *J. Geophys. Res.*, **104**, 30 937-30 946.

Baldwin, M.P., and T.J. Dunkerton, 2001: Stratospheric Harbingers of Anomalous Weather Regimes. *Science*, **294**, 581-584.

Duchon, C. E., 1979: Lonczos filtering in one and two dimensions. J. Appl. Met. **18**, 1016-1022.

Efron, B. 1979: Bootstrap methods: another look at the jackknife. Ann. Statist., **7**, 1-26.

Rayner, N.A., D.E. Parker, E.B. Horton, C. K. Folland, L. V. Alexander, D. P. Rowell, E.C. Kent, and A. Kaplan, 2003: Global analyses of sea surface temperature, sea ice, and night marine air temperature since the late nineteenth century. J. Geophys. Res. **108**, No. D14, 4407, doi:10.1029/2002JD002670, 2003.

Holopainen, E. O., L. Rontu, and N. C. Lau, 1982: The effect of large-scale transient eddies on the time-mean flow in the atmosphere. J. Atmos. Sci., **39**, 1972-1984.

Kalnay, E. and coauthors, 1996: The NCEP/NCAR 40-Year Reanalysis Project. Bull. Amer. Meteor. Soc., **77**, 437-471.

Kodera, K., H. Koide, H. Yoshimura, 1999: Northern Hemisphere winter circulation associated with the North Atlantic Oscillation and stratospheric polar-night jet *Geophys. Res. Lett.*, **26**, 443-446.

Kodera, K., Y. Kuroda, and S. Pawson, 2000: Stratospheric sudden warmings and slowly propagating zonal-mean zonal wind anomalies, *J. Geophys. Res.*, **105**, 12351-12359.

Kuroda, Y., and K. Kodera, 1999: Role of planetary waves in the stratosphere-troposphere coupled variability in the northern hemisphere winter *Geophys. Res. Lett.*, **26**, 2375-2378.

Quadrelli, R., and J.M. Wallace, 2002: Dependence of the structure of the Northern Hemisphere Annular Mode on the polarity of ENSO. *Geophys. Res. Letts.*, **29**, doi:10.1029/2002GL015807.

Takaya, K. and H. Nakamura, 1997: A formulation of a wave-activity flux for stationary Rossby waves on a zonally varying basic flow. Geophys. Res. Lett., **24**, 2985-2988.

Takaya, K. and H. Nakamura, 2001: A formulation of a phase-independent wave-activity flux for stationary and migratory quasi-geostrophic eddies on a zonally-varying basic flow. J. Atoms. Sci., **58**, 608-627.

Thompson, D. W. and J.M. Wallace, 1998: The arctic oscillation signature in the wintertime geopotential height. *Geophys. Res. Lett.*, **25**, 1297-1300.

Thompson, D. W. and J.M. Wallace, 2000: Annular modes in the extratropical circulation. Part I: Month-to-month variability. J. Climate., **13**, 1000-1016.

ENSO サイクルに伴う北半球環状モードの成層圏－対流圏結合過程の変調

塩竈秀夫・向川均

要旨

近年，季節内変動スケールの北半球環状モードが対流圏で観測される際，成層圏からの西風偏差下方伝播が先立って観測されることが，いくつかの観測的研究によって示されてきた．本研究では，長期間の観測データを用いることで，この種の成層圏－対流圏結合過程が ENSO サイクルの warm フェーズと cold フェーズでどのように変調するかを調べた．

成層圏での西風偏差下方伝播過程は ENSO サイクルによらずに観測されたが，その際に主に寄与する惑星波は異なり，WN 2（cold）と WN 1 (warm)であった．上向き波活動度フラックス偏差が観測される経度帯も cold フェーズではユーラシア領域，warm フェーズでは PNA 領域であった．成層圏での西風偏差の後に対流圏で西風偏差が観測されるのは，cold フェーズだけたっだ．この時，WN 2 と総観規模擾乱の運動量輸送偏差が対流圏偏差場の形成に寄与した．

キーワード: 環状モード，成層圏－対流圏結合過程, ENSO, 突然昇温